Fuzzy Sliding Mode Controller Based Trajectory Tracking Control of Free Flying Space Robot Manipulator System

Esubalew W. Shibabw(✉) and Gerbaw Y. Tamiru

Bahirdar Institute of Technology, Bahirdar University, Bahir Dar, Ethiopia
esubalewwalle378@gmail.com

Abstract. A free flying space robot manipulator system (FFSRMS) is made up of a six degrees of freedom (DOF) spacecraft and n degree of freedom manipulator mounted on the base spacecraft. The space robot manipulator is used to perform a variety of tasks in space or on orbit service (OOS), such as assembling and repairing spacecraft, refueling satellites in orbit, and removing space debris. Unlike ground-based robot manipulators, a space robot manipulator has no fixed base. As a result, the base and manipulator are strongly coupled. Furthermore, the system operates in unstructured and zero gravity environment. The kinematics and dynamics of a FFSRMS has been developed based on chaseles theorem and Euler-Lagrangian equation of motion respectively. The stability of the system and the convergence of the tracking errors to the origin has been checked using Lyapunov stability criterion. This work used a fuzzy sliding mode controller (FSMC) to examine a space robot manipulator trajectory tracking control capability in joint space and robustness. The proposed controller has been simulated in MATLAB/Simulink considering external disturbance and parametric variation and compared with the sliding mode controller to evaluate how effective it is. The results reveal that the proposed controller is robust and has good trajectory tracking capability with a reduced Integral Time Absolute Error (ITAE) and it eliminate the chattering effect. The comparative study shows that FSMC has reduced ITAE than SMC.

Keywords: FFSRMS · FSMC · OOS · Robust · Trajectory tracking

1 Introduction

Space robotic manipulator technology is the new frontier field of study which attracts the attention of many countries to take space power and a subsequent study has been conducted over the past 40 years. Space robotic manipulator plays a significant role for servicing a spacecraft after they are deployed on orbit (OOS) that would prolong the life span of a spacecraft and would be too risky and time consuming if performed by an astronaut, such as assembling,

B. H. Woldegiorgis et al. (Eds.): ICAST 2022, LNICST 455, pp. 137–158, 2023.
https://doi.org/10.1007/978-3-031-28725-1_9

constructing or repairing a space station in orbit [1], on orbit refueling [2], space debris removal [3,4] and extravehicular activity(EVA) support [1].

The historical development and advancement of space robotic manipulator was presented in [5]. Shuttle Remote Manipulator System (SRMS) also known as canadarm1 was the first manipulator mounted on space shuttle orbiter on second mission of the space shuttle (STS-2) to capture Hubble Space Telescope (HST) and to positioning astronauts during extravehicular activity (EVA) in 1981. There are some other robotic manipulator mounted on international space station (ISS) such as; Space Station Remote Manipulator System (SSRMS) also known as canadarm2, the Japanese Experiment Module Remote Manipulator System (JEMRMS), European Robotic Arm (ERA), Robonaut1 and Robonaut2 [8].

In order to capture a target spacecraft, a series of stages must be taken. The first step is planning of how the robot arm should capture the target spacecraft by observing the motion and collecting information about the physical property of the target spacecraft using different sensors like vision, radar sensors. The second stage is controlling the base spacecraft to move to the capturing location (for free flying case) such that, the manipulator is ready to grasp the target satellite. The third step is the actual capturing of the target space robot by the end effector. Lastly, the captured spacecraft is stabilized along with the capturing satellite manipulator by considering the servicing and target spacecraft as one system, this is called post capturing stage [8].

An accurate and precise trajectory tracking of space robot is required when the space robot manipulator is commanded to capture some target spacecraft or object. However, unlike ground-based robot manipulator, space robot has no fixed base, which makes the system dynamics strongly coupled and difficult to formulate both the kinematic and dynamic motion of the space robot manipulator system accurately and to design the controller. In addition, the space robot is working in zero gravity and unstructured environment. Moreover, to cope up external disturbances and parametric variations due to, thrust firing and additional payload carried by the manipulator, a robust controller is required. Many scholars have proposed different path planning algorithm and controller scheme for space robot manipulator system. Researchers in [10–13] presented adaptive controller as a feasible solution to overcome the following two problems: The dynamic equation of the system cannot linearly parameterized and the uncertainty in kinematic mapping from inertial space to joint space when the base is free floating. Gu You-Liang and Yangsheng Xu [10] proposed a normal augmentation approach to adaptive control by modeling the entire free floating space robot system as extended robot. The simulation result shows that the proposed controller asymptotically stabilized the space robot manipulator system to track a given trajectory in Cartesian space. However, the proposed approach requires large computation and it requires measurement of spacecraft accelerations. To alleviate the drawback in [10], Parlaktuna et al. [11] proposed an adaptive controller based on an extended robot approach and an on-line adaptive estimation law for an unknown parameter along with a computed torque controller. Sim-

ulation of a two link planner space robot system is conducted using MATLAB and the simulation result shows that the proposed controller has a good position trajectory tracking performance. However, the algorithm that the authors follow to eliminates the measurement of acceleration requires, a large computation.

In [12], the parameterization problem of dynamic equation and adaptive control of free floating space robot are discussed. Abiko et al. [13] proposed adaptive control of fully free floating space robot with dynamic and kinematic model uncertainty. The authors discussed adaptive control for a torque controlled space robot without acceleration measurement. Limin Xie et al. [14] proposed a robust fuzzy slide mode controller for controlling the free floating space robot manipulator system, so that it can correctly track the required trajectory while also suppressing vibration induced by the flexible joints and flexible link. The simulation, however, is conducted in two dimension with two-link manipulator. Meanwhile, the error convergence speed is also slow. Yicheng Liu et al. [15] proposed trajectory tracking for a dual arm free floating space robot with a class of general non-singular predefined time terminal sliding mode. Simulation using MATLAB has been conducted to check the performance of the control and the simulation result shows that the joint angles successfully track the given trajectory. However terminal slide mode controller has chattering problem for bounded random-changing external disturbances. In order to solve this problem, the authors adopt a continuous function scheme at the cost of high gain.

Xin Zhang et al. [16] proposed adaptive robust decoupling control of multi-arm space robots using time delay estimation technique. The paper is focused on decoupling and counteracting the coupling between the base and the manipulator. The simulation is conducted using MATLAB for decoupling control of multi-arm space robot and they have made comparative analysis of computed torque control (CTC) based SMC and time delay estimation (TDE) based SMC and the result demonstrates that the TDE based SMC with a reduced time delay length still achieve a guaranteed control performance. However, the measure taken to reduce the effect of chattering problem of SMC controller is replacing the switching control action by saturation control action operated based on the boundary layer width. Meanwhile, the authors select the boundary layer width randomly (they do not use optimal selection algorithm.) because, if the boundary layer width variable is selected as large the control input will be smooth, but the robustness of the controller degrade, which may causes a steady-state error. Shiyuan Jia and Jin J. Shan [17], presented a trajectory tracking control of space manipulator in the presence of actuator uncertainties, such as actuator fault, actuator saturation and the bias control torque. In addition they have considered parametric uncertainty and external disturbance. In order to resolve the problem mentioned, the authors applies a continuous integral slide mode controller for trajectory tracking control of the space robot manipulator.

This paper focused on trajectory planning and tracking control of free flying space robot manipulator and stabilization of base spacecraft position and orientation using fuzzy slide mode controller. The attitude of base spacecraft is represented using Euler angles. The fifth order polynomial trajectory plan-

ning technique is adopted for the manipulator joint and spacecraft attitude desired trajectory. A slide mode controller is a robust controller that can compensate external disturbance and parameter uncertainty change in the system while maintaining the manipulator tracks it's given trajectory with a minimum error and fast convergence. However, SMC suffers a chattering problem due to a high frequency switching control law, in order to alleviate this problem, we adopt a fuzzy logic controller.

The main contributions of this paper are:

1. A fuzzy sliding mode controller is designed for trajectory tracking control of a free flying space robot manipulator system that allows the manipulator to track the desired trajectory with a minimum error and that can reject an external disturbances and parameter uncertainties while the base spacecraft positions and orientations are stabilized in a desired position with a minimum errors.
2. Most of the above mentioned research works such as [14,16,17] analyzed the performance of their controller in 2D plane. However, for real space mission a 3D motion analysis and response is required. So, we are conducted a 3D simulation of a 9 DOF (Six for base positions and attitudes, three for the manipulator joint angles) free flying space robot.
3. As most studies point out, controlling all of the $6+n$ DOF without decoupling the system dynamics is difficult, especially for a free-flying space robot, where the base spacecraft and the manipulator are strongly coupled. This paper, however, uses no decoupling strategies.

2 Modeling of Space Robot Manipulator System

2.1 Assumptions

The formulation of kinematics and dynamic motion of a free flying space robot manipulator system requires the following assumptions.

1. The space robot manipulator system is assumed to be rigid and works in micro-gravity or no gravity environment ($g = 0$).
2. The orbital mechanics is not considered (the body frame is assumed to be aligned with the orbiting frame).
3. As explained in [19], there are several external disturbance torques acting on spacecraft in orbit. In this paper all the disturbances considered are assumed to be bounded.

2.2 Kinematics of Space Robot Manipulator System

A spacecraft equipped with a single n rigid links connected by a revolute joints is shown in Fig. 1. The base spacecraft is defined as link 0, with joint 0 coinciding at the space robot base center of mass. The end- effector is located at a virtual

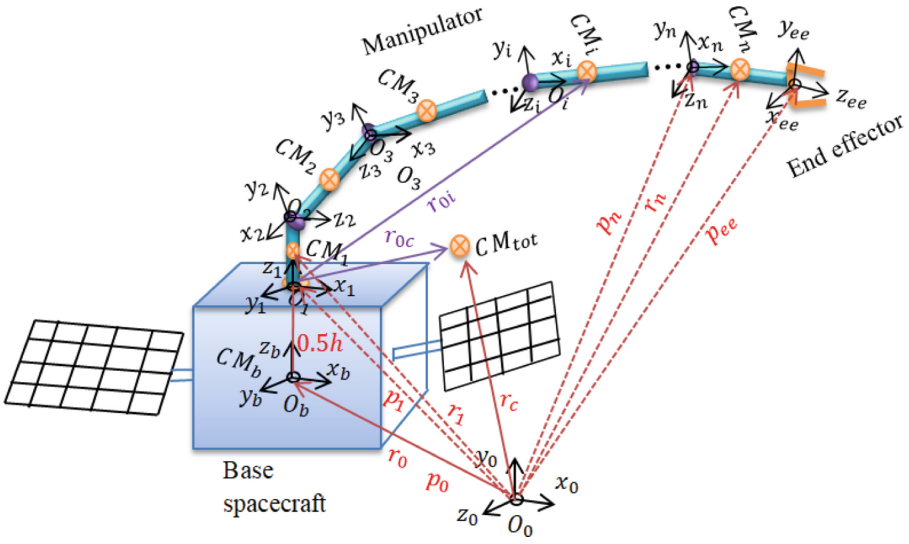

Fig. 1. Geometry of a free flying space robot manipulator system

joint $n+1$. For ground base robot manipulator system, the relationship between these two spaces is non-linear. However, as mentioned in [20], the position and orientation of the end effector of a free flying space robot manipulator may not have a closed form solution, since the motion of the end effector depends on the past history of the manipulator motion. This makes difficult to formulate the inverse kinematics. Thus, the kinematics is formulated at velocity level.

To develop the kinematics of FFSRMS, we use four coordinate systems; An inertial coordinate system with origin Ω, body coordinate system located at the center of mass of the base spacecraft with origin Q_b, a set of $n+1$ joint fixed coordinate systems J_i with origin, $Q_i (i = 0 : n+1)$, and a set of n link fixed coordinate systems, L_i located at the center of mass of each link. The orientation of the base spacecraft with respect to the inertial frame is expressed in Euler angle specified by a rotation matrix in Eq. (1). In order to be free of singularity we would prefer to choose roll-pitch-yaw (ϕ, θ, ψ) rotation sequence [22].

$$R_{0b} = R_\phi R_\theta R_\psi = \begin{bmatrix} 1 & 0 & 0 \\ 0 & c\phi & -s\phi \\ 0 & s\phi & c\phi \end{bmatrix} \begin{bmatrix} c\theta & 0 & s\theta \\ 0 & 1 & 0 \\ -s\theta & 0 & c\theta \end{bmatrix} \begin{bmatrix} c\psi & -s\psi & 0 \\ s\psi & c\psi & 0 \\ 0 & 0 & 1 \end{bmatrix}$$

$$R_{0b} = \begin{bmatrix} c\psi c\theta & c\psi s\theta s\phi - s\psi c\phi & s\psi s\phi + c\psi s\theta c\phi \\ s\psi c\psi & s\psi s\theta s\phi + c\psi c\phi & s\psi s\theta c\phi - c\psi s\phi \\ -s\theta & s\theta s\phi & s\theta c\phi \end{bmatrix} \tag{1}$$

The body fixed angular velocity $(\omega_x, \omega_y, \omega_z)$ is related to the Euler angle rate by;

$$\begin{bmatrix} \omega_x \\ \omega_y \\ \omega_z \end{bmatrix} = \begin{bmatrix} 1 & 0 & s\theta \\ 0 & c\phi & s\phi c\theta \\ 0 & -s\phi & c\phi s\theta \end{bmatrix} \begin{bmatrix} \dot{\phi} \\ \dot{\theta} \\ \dot{\psi} \end{bmatrix} \tag{2}$$

where, the notation c and s is for cosine and sine of the respected Euler angle. The rotation matrix of the manipulator, ${}^{i}R_{i-1}$ from joint J_i to joint J_{i-1} is built using Denavit-Hartenberg (DH) convention as specified in [23]. In this convention the transformation matrix, T_i is represented as a product of four basic transformation with four DH parameters. θ_i,l_i,α_i, and d_i as shown in Table 1

$$T_i = (rot_{z,\theta_i})(trans_z, d_i)(trans_x, l_i)(rot_{x,\alpha_i})$$

$$T_i = \begin{bmatrix} c\theta_i & -s\theta_i c\alpha & s\theta_i s\alpha & l_i c\theta_i \\ s\theta_i & c\theta_i c\alpha & -c\theta_i s\alpha & l_i s\theta_i \\ 0 & s\alpha & c\alpha & d_i \\ 0 & 0 & 0 & 1 \end{bmatrix} \tag{3}$$

Consider Fig. 1, the position of the end-effector p_e, is given by;

Table 1. DH parameters and their geometric meaning.

DH parameters	Name	Geometric meaning
θ_i	Joint angle	Rotation from ${}^{x}J_i$ to ${}^{x}J_{i+1}$about ${}^{z}J_i$
l_i	Link length	Distance along the common normal between ${}^{z}J_i$ and ${}^{z}J_{i+1}$
α_i	Link offset	Rotation from ${}^{z}J_i$ to ${}^{z}J_{i+1}$about ${}^{x}J_{i+1}$
d_i	Link twist	Distance between O_i and ${}^{x}J_{i+1}$ along ${}^{z}J_i$

$$p_e = r_0 + b_0 + \sum_{i=1}^{n} l_i \tag{4}$$

Where, r_0, b_0, l_i are the position of center of mass of base spacecraft, the position of first joint coordinate system with respect to spacecraft center of mass and length of link i respectively.

By derivating Eq. (4) and substituting Eq. (8) and (9) on it, the linear and angular velocity of the end effector is given as;

$$\begin{bmatrix} v_e \\ \omega_e \end{bmatrix} = \begin{bmatrix} v_b \\ \omega_b \end{bmatrix} + \begin{bmatrix} \omega_b \times (p_e - r_0) + \sum_{j=1}^{n} (k_j \times (p_e - p_j))\dot{\theta}_j \\ \sum_{j=1}^{n} \left(k_j \dot{\theta}_j\right) \end{bmatrix} \tag{5}$$

Where, v_b and ω_b are the linear and angular velocity of the base spacecraft respectively, k_j is he rotation axis of the i^{th} revolute joint usually defined as

the z axis in the corresponding link frame, $\dot{\theta}_j$ denotes the angular velocity of i^{th} rotational joint. Equation (5) can be expressed in canonical form as:

$$\begin{bmatrix} v_e \\ \omega_e \end{bmatrix} = \left[J_s \dot{\phi} + J_m \dot{\theta} \right] \tag{6}$$

Where, $\dot{\phi} = [v_b, \omega_b]^T$ is the generalized linear and angular velocity vector of the base spacecraft, $\dot{\theta} = [\dot{\theta}_1, \dot{\theta}_2 \ldots \dot{\theta}_n]$ are joint angular velocities. $J_s \in R^{6\times 6}$ is the Jacobian of the base spacecraft, $J_m \in R^{6\times n}$ is the standard Jacobian of a ground base robot manipulator.

$$J_s = \begin{bmatrix} I_{3,3} & -(p_e - r_0)^{\times} \\ 0_{3,3} & I_{3,3} \end{bmatrix}, J_m = \begin{bmatrix} k_1 \times (p_e - p_1) \ldots k_i \times (p_e - p_i) & 0_{3,n-i} \\ k_1 \ldots k_i & 0_{3,n-i} \end{bmatrix}$$

The notation $r^{\times}$ is used to denote the skew symmetric matrix associated with the vector $r = [r_x, r_y, r_z]^T$ can be written in matrix form as [24].

$$r^{\times} = \begin{bmatrix} 0 & -r_z & r_y \\ r_z & 0 & -r_x \\ -r_y & r_x & 0 \end{bmatrix}$$

2.3 Dynamics of Space Robot Manipulator System

The equation of motion of a free flying space robot manipulator system as shown in Fig. 1 is formulated using Euler-Lagrangian equation of motion. The potential energy is set to zero, as it is mentioned on assumption 1. Hence, the Lagrangian (L) is equals to the system kinetic energy (T).

$$L = T = \frac{1}{2} \left(\sum_{i=0}^{n} \left(\omega_i^T I_i \omega_i + m_i v_i^T v_i \right) \right) \tag{7}$$

where,

$$v_i = v_b + \omega_b^{\times} (r_i - r_0) + \sum_{j=1}^{i} \left(k_j^{\times} (r_i - p_j) \dot{\theta}_j \right) \tag{8}$$

$$\omega_i = \omega_b + \sum_{j=1}^{i} \left(k_j \dot{\theta}_j \right) \tag{9}$$

Substituting Eq. (8) and (9), into Eq. (7) yields;

$$\begin{aligned} L = \frac{1}{2} \left(\omega_b^T I_b \omega_b + m_b v_b^T v_b \right) + \frac{1}{2} \left(\omega_b + \sum_{j=1}^{i} k_j \dot{\theta}_j \right)^T I_i \left(\omega_b + \sum_{j=1}^{i} k_j \dot{\theta}_j \right) \\ + \frac{1}{2} m_i \left(v_b + \omega_b \times (r_i - r_0) + \sum_{j=1}^{i} (k_j \times (r_i - p_j)) \dot{\theta}_j \right)^T \\ \left(v_b + \omega_b \times (r_i - r_0) + \sum_{j=1}^{i} (k_j \times (r_i - p_j)) \dot{\theta}_j \right) \end{aligned} \tag{10}$$

By proper re-arrangement and simplification of Eq. (10) we will get;

$$L = T = \frac{1}{2}\begin{bmatrix} v_b^T & \omega_b^T & \dot{\theta}_i^T \end{bmatrix}\begin{bmatrix} H_v & H_{v\omega} & H_{vm} \\ H_{\omega v} & H_{\omega} & H_{\omega m} \\ H_{mv} & H_{m\omega} & H_m \end{bmatrix}\begin{bmatrix} v_b \\ \omega_b \\ \dot{\theta}_i \end{bmatrix} \tag{11}$$

where,

$$H_v = m_{tot}(I_{3,3})$$

$$H_{v\omega} = -\sum_{i=1}^{n} m_i r_{0i}^{\times}$$

$$H_{vm} = \sum_{i=1}^{n}(m_i J_{Ti})$$

$$H_{\omega} = I_0 + \sum_{i=1}^{n}(I_i - m_i r_{0i}^{\times} r_{0i}^{\times})$$

$$H_{\omega m} = \sum_{i=1}^{n}(I_i J_{Ri} + m_i r_{0i} J_{Ti})$$

$$H_{\omega v} = H_{v\omega}^T$$

$$H_{\omega m} = H_{m\omega}^T$$

$$H_{mv} = H_{vm}^T$$

$$H_{m\omega} = H_{\omega m}^T$$

$$H_m = \sum_{i=1}^{n} J_{Ri}^T I_i J_{Ri} + m_i J_{Ti}^T J_{Ti}$$

$$J_{\mathrm{Ti}} = \begin{bmatrix} k_1{}^{\times}(r_i - p_1) \ldots k_i{}^{\times}(r_i - p_i) & 0_{3,n-i} \end{bmatrix}, \forall\ (1 \le i \le n)$$

$$J_{\mathrm{Ri}} = \begin{bmatrix} k_1{}^{\times} \ldots\ \mathrm{k}_i{}^{\times}\ 0_{3,n-i} \end{bmatrix},\ \forall\ (1 \le i \le n)$$

The i^{th} link moment of inertia matrix with respect to inertial frame of reference is given by;

$$I_i = R_{Li}{}^{CM} I_i R_{Li}^T \tag{12}$$

where, ${}^{CM}I_i$ is moment of inertia at center of mass. Now select the manipulator joint angle vector, q and the spacecraft linear and angular position vector, $\dot{x}_b = [v_b^T, \omega_b^T]$ as a generalized coordinate, Eq. (11) can be re-written as;

$$L = T = \frac{1}{2}\begin{bmatrix} \dot{x}_b^T & \dot{q}_i^T \end{bmatrix}\begin{bmatrix} H_b & H_{bm} \\ H_{bm}^T & H_m \end{bmatrix}\begin{bmatrix} \dot{x}_b \\ \dot{q}_i \end{bmatrix} \tag{13}$$

$$H_b = \begin{bmatrix} H_v & H_{v\omega} \\ H_{\omega v}^T & H_{\omega} \end{bmatrix}$$

$$H_{bm} = \begin{bmatrix} H_{v\omega}^T \\ H_{\omega m}^T \end{bmatrix}$$

Where, $H_b \in \mathbb{R}^{6\times 6}$,$H_m \in \mathbb{R}^{n\times n}$, are the inertia matrix of the spacecraft and the manipulator respectively, $H_{bm} \in \mathbb{R}^{6\times n}$, is the dynamic coupling inertia matrix, which represent the contribution of the manipulator to the base spacecraft and vice-versa: J_{Ti}, J_{Ri}, are the linear velocity and the angular velocity Jacobian matrix for the i^{th} link center of mass respectively. Simplifying Eq. (13) will give as;

$$L = \frac{1}{2}\dot{x}_b^T H_b \dot{x}_b + \frac{1}{2}\dot{x}_b^T H_{bm}\dot{x}_b + \frac{1}{2}\dot{q}^T H_m \dot{q} + \frac{1}{2}\dot{q}^T H_{bm}^T \dot{q} \tag{14}$$

The Euler-Lagrangian equation of motion is given by;

$$\frac{d}{dt}\left(\frac{\partial L}{\partial \dot{x}_b}\right) - \left(\frac{\partial L}{\partial x_b}\right) = \begin{bmatrix} f_b \\ \tau_b \end{bmatrix} \tag{15}$$

$$\frac{d}{dt}\left(\frac{\partial L}{\partial \dot{q}}\right) - \left(\frac{\partial L}{\partial q}\right) = \tau_m \tag{16}$$

Now apply Euler-Lagrangian equation of motion onto Eq. (14) will result the dynamic equation of motion of a free flying space robot manipulator system given in Eq. (17)

$$\begin{bmatrix} H_b & H_{bm} \\ H_{mb} & H_m \end{bmatrix} \begin{bmatrix} \ddot{x}_b \\ \ddot{q} \end{bmatrix} + \begin{bmatrix} \dot{H}_b & \dot{H}_{bm} \\ \dot{H}_{mb} & \dot{H}_m \end{bmatrix} \begin{bmatrix} \dot{x}_b \\ \dot{q} \end{bmatrix} - \begin{bmatrix} C_b \\ C_m \end{bmatrix} = \begin{bmatrix} f_b \\ \tau_b \\ \tau_m \end{bmatrix} \tag{17}$$

With,

$$C_b = \frac{1}{2}\frac{\partial}{\partial x_b}(\dot{x}_b^T H_b \dot{x}_b + \dot{x}_b^T H_{bm}\dot{x}_b + \dot{q}^T H_m \dot{q} + \dot{q}^T H_{bm}^T \dot{q})$$

$$C_m = \frac{1}{2}\frac{\partial}{\partial q}(\dot{x}_b^T H_b \dot{x}_b + \dot{x}_b^T H_{bm}\dot{x}_b + \dot{q}^T H_m \dot{q} + \dot{q}^T H_{bm}^T \dot{q})$$

Equation (17) can be expressed in a canonical form as;

$$H\ddot{\varphi} + C\dot{\varphi} = \tau \tag{18}$$

With,

$$C = \dot{H} - \begin{bmatrix} C_b \\ C_m \end{bmatrix}$$

Where, $\ddot{\varphi} = [\ddot{x}_b, \ddot{q}]^T$ is a generalized acceleration vector and $\tau = [f_b, \tau_b, \tau_m]^T$ is a generalized force and torque vector term.

3 Controller Design

In this section, a free flying space robot manipulator control system based on a fuzzy sliding mode controller is designed in such away that, the manipulator

can track a desired trajectory in joint space, while the position and attitude of the base spacecraft are stabilized in the direction that guarantee communication with ground station. If we take into account disturbances and uncertainty, the dynamic model given in Eq. (18) is modified to;

$$H\ddot{\varphi} + C\dot{\varphi} + \tau_d + \Delta u = \tau \tag{19}$$

$\tau_d = [\tau_{d1}, \tau_{d2} \ldots \tau_{dn}]^T$ represents the bounded disturbance force or torque vector applied on base spacecraft($|\tau_d| \leq d_i$) and manipulator,Δu denotes the bounded uncertainty dynamics. i.e.,$|\Delta u| \leq u_i$.

Lemma 1. *The inertial matrix H and the Coriolis force C in Eq. (19) are bounded with* $\lambda I_{n,n} \leq H \leq \lambda_{max} I_{n,n}$ *and* $||C|| \leq ||c\dot{\varphi}||$, *where* λ,λ_{max} *and c are positive constants [25].*

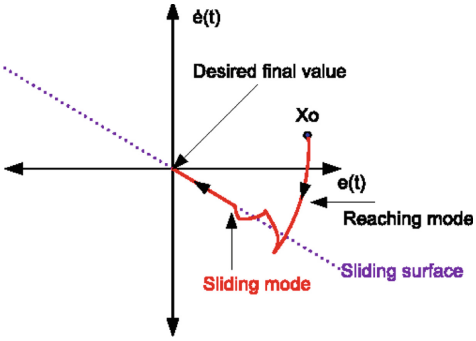

Fig. 2. Sliding surface manifold [27]

3.1 Sliding Mode Controller Design

SMC is one of the variable structure control system (VSCS) approaches. VSCS is a variable high-frequency switching controller [26]. Designing of a slide mode controller (SMC) majorly consists of two procedure;

1. Select sliding surface vector as;

$$s = \dot{e} + K_p e + K_i \int_0^t e(\tau) d\tau \tag{20}$$

Where, K_p,K_i are a diagonal and positive definite matrix (sliding surface gains), e,$\dot{e} \in \mathbb{R}(6 + n \times 1)$ are an error and rate of error vectors respectively, and they are given as follow;

$$e = \varphi_{di} - \varphi_i \tag{21}$$

$$\dot{e} = \dot{\varphi}_{di} - \dot{\varphi}_i \tag{22}$$

Where, $\varphi_{di}, \dot{\varphi}_{di}$ are desired linear, angular position and velocity of base and the manipulator respectively. $\varphi_i = [x, y, z, \phi, \theta, \psi, \theta_1, \theta_2, \ldots, \theta_n]$ are the actual base position and attitude and manipulator joint angles. Differentiating Eq. (20) with respect to time yields;

$$\dot{s} = \ddot{e} + K_p\dot{e} + K_i e \tag{23}$$

Solving for φ_i in Eq. (20), then substitute it with Eq. (22) into Eq. (23) and set $\dot{s} = 0$ in Eq. (23), the equivalent control law can be obtained as;

$$\tau_{eqv} = H(\ddot{\varphi}_{di} + K_p\dot{e} + K_i e) + C\dot{\varphi} + \tau_d + \Delta_u \tag{24}$$

Where, τ_{eqv} is the equivalent control law, considering disturbance and uncertainty that makes the system trajectory moving on the sliding surface as indicated in Fig. 2.

2. Select an appropriate reaching control law. In this work, a constant plus proportional reaching control law is adopted as expressed in Eq. (25).

$$\dot{s} = -K_s s - Gsgn(s) \tag{25}$$

Where, G, K_s are a diagonal and positive definite matrix switching gains and reaching control law gains respectively. $sgn(s)$ denote a signum function.

$$sgn(s) = \begin{cases} -1, & if\ s < 0 \\ 1, & if\ s > 0 \end{cases}$$

Finally, the total control law can be obtained as;

$$\tau_{tot} = \tau_{eqv} + H(Gsgns + K_s s) + \tau_d + \Delta_u \tag{26}$$

3.2 Fuzzy Logic Controller Design

In this subsection, a fuzzy logic controller based on zero order Sugeno inference mechanism is designed. The control law expressed in Eq. (26) suffers with chattering problem due, to a high frequency switching control law represent by $Gsgn(s)$.

In this paper, a singleton MF is used for the output variable since, it improves the efficiency of the defuzzification process or simplifies the computation required by the Mamdani method, that finds the centroid of a two dimensional function instead of integrating across the two dimensional function to find the centroid, it is better to use the weighted average of a few data points.

$$-Gsgn(s) = -G\Delta u \tag{27}$$

Now a fuzzy logic controller can be design to smooth the switching controller expressed in Eq. (27) with a FLC output Δu.

1. **Fuzzify Inputs:** Firstly, the sliding surfaces, s and the fuzzy logic controller outputs, Δu has taken as input and output variables of fuzzy inference system respectively. Then, a triangular and a singleton membership functions are assigned for fuzzy input and output variables respectively, as shown in Fig. (3) with a seven linguistic variables; Negative Large (NL), Negative Medium (NM), Negative Small (NS), Zero (Z), Positive Large (PL), Positive Medium (PM) and Positive Small (PS). The range of input and output variables has taken from $[-5\ 5]$. Additionally, the width of both input and output fuzzy MF $\beta = \frac{5}{3}$, as shown in Fig. 3a & 3b.

Remark 1. The input MF range is selected based on the range sliding surfaces from SMC simulation result and the output MF range is based on the range of signum function (since, FLC is chosen to substitute the switching control law of SMC and to produce a continuous control signal as shown in Fig. 3c.

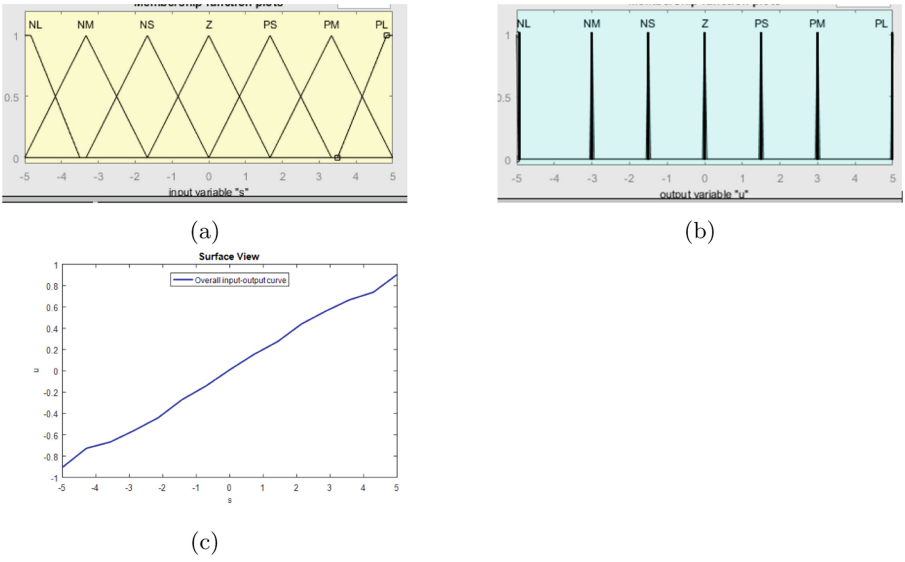

(a) (b)

(c)

Fig. 3. Membership function of input and output of fuzzy logic controller:(a) Input membership function, (b) Output membership function (c) Overall input output curve

2. **Fuzzy rule construction:** The fuzzy rules are designed based on the methodology that the high frequency switching control law have direct and positive relationship with sliding manifold.
   if **s** is NL, then Δu is NL
   if **s** is NM, then Δu is NM
   if **s** is NS, then Δu is NS
   if **s** is Z, then Δu is Z

if **s** is PS, then Δu is PS
if **s** is PM, then Δu is PM
if **s** is PL, then Δu is PL

3. Computing the output of fuzzy logic controller as;

$$-G\Delta u = -G\sum_{i=-5}^{5}\frac{\mu_i(s)i}{\mu_i(s)} \tag{28}$$

where, $\mu_i(s)$ is the strength of the i^{th} rule and i is the associated single membership function of Δu

3.3 Trajectory Planning

In this study, a fifth order polynomial path planning technique is adopted to plan the desired trajectory of the space robot base attitude and manipulator joint position.

$$\dot{\varphi}_i(t) = a_1 + 2a_2t + 3a_3t^2 + 4a_4t^3 + 5a_5t^4 \tag{29}$$

The velocity and acceleration can be obtained by taking the first & second derivative of Eq. (29) respectively.

$$\dot{\varphi}_i(t) = a_1 + 2a_2t + 3a_3t^2 + 4a_4t^3 + 5a_5t^4 \tag{30}$$

$$\ddot{\varphi}_i(t) = 2a_2 + 6a_3t + 12a_4t^2 + 20a_5t^3 \tag{31}$$

where $t_0 \leq t \leq t_f$ and a_i, for $i = 0, 1 \ldots 5$ are coefficients of the polynomial and determined by solving the following polynomial equation. the a_i parameter can be found as;

$$\begin{bmatrix} a_0 \\ a_1 \\ a_2 \\ a_3 \\ a_4 \\ a_5 \end{bmatrix} = \begin{bmatrix} 1 & t_0 & t_0^2 & t_0^3 & t_0^4 & t_0^5 \\ 0 & 1 & 2t_0 & 3t_0^2 & 4t_0^3 & 5t_0^4 \\ 0 & 0 & 2 & 6t_0 & 12{t_0}^2 & 20{t_0}^3 \\ 1 & t_{tf} & t_{tf}^2 & t_{tf}^3 & t_{tf}^4 & t_{tf}^5 \\ 0 & 1 & 2t_{tf} & 3t_{tf}^2 & 4t_{tf}^3 & 5t_{tf}^4 \\ 0 & 0 & 2 & 6t_{tf} & 12t_{tf}^2 & 20t_{tf}^3 \end{bmatrix}^{-1} \begin{bmatrix} \varphi_i\,(0) \\ 0 \\ 0 \\ \varphi_i\,(\mathrm{tf}) \\ 0 \\ 0 \end{bmatrix}$$

4 Stability Analysis

In this section the stability of the designed controller is proved using Lyapunov function technique (Fig. 4). Select a lyapunov function candidate as;

$$V = \frac{1}{2}s^T s \tag{32}$$

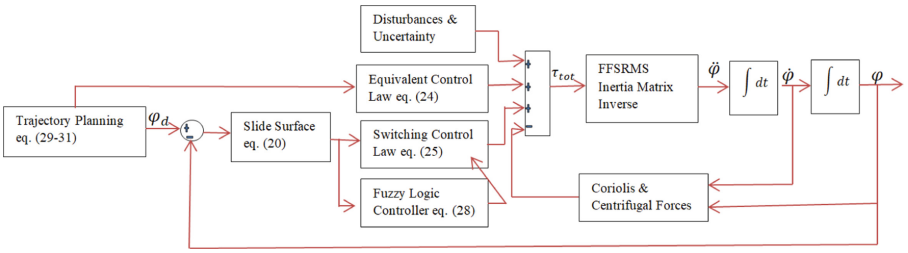

Fig. 4. Overall control system structure

Differentiating Eq. (32) with respect to time and substituting Eq. (19) and (26) into it gives;

$$\begin{aligned}
\dot{V} &= s^T \dot{s} \\
&= s^T(\ddot{\varphi}_{di} - \ddot{\varphi}_i + K_p\dot{e} + K_i e) \\
&= s^T(\ddot{\varphi}_{di} - H^{-1}(\tau_{tot} - C\dot{\varphi} - \tau_d - \Delta_u) + K_p\dot{e} + K_i e) \\
&= s^T(\ddot{\varphi}_{di} - H^{-1}(\tau_{eqv} + G\Delta_f + K_s s - C\dot{\varphi} - \tau_d - \Delta_u) + K_p\dot{e} + K_i e) \\
&= s^T H^{-1}\left(-G\Delta_f - K_s s + \tau_d + \Delta_u\right) \\
&= s^T(H^{-1}(\tau_d + \Delta_u) - |s^T|H^{-1}(G) - s^T H^{-1} K_s s
\end{aligned} \tag{33}$$

By choosing appropriate values G and K_s which satisfy $\dot{V} \leq 0$ and the matrix H^{-1} is positive definite, Eq. (33) is always less than zero. Therefore the stability is proven.

5 Simulation Results and Discussion

In this section, simulation of three link free flying space robot as shown in Fig. (5) is conducted using MATLAB. The initial and terminal time for trajectory planing is set as $t_0 = 0$ and $t_f = 20$ second respectively. The inertia and DH parameters of a FFSRMS are specified in Table 2 and Table 3 respectively.

Table 2. Kinematic ad dynamic parameters of the FFSRMS [29]

	$m(kg)$	$l(m)$	$a(m)$	$b(m)$	$I_{xx}(kgm^2)$	$I_{yy}(kgm^2)$	$I_{zz}(kgm^2)$
Base	100	–	–	0.5	30	30	30
Link1	8	0.5	0.25	0.25	0.2	0.0064	0.2
Link2	10	1	0.5	0.5	0.008	0.8	0.8
Link3	10	1	0.5	0.5	0.008	0.8	0.8

Table 3. DH parameters of the FFSRMS

	$\alpha(rad)$	$l(m)$	$d(m)$	$\theta(rad)$
Link1	0.5π	0.5	0.5	θ_1
Link2	0	1	0	θ_2
Link3	0	1	0	θ_3

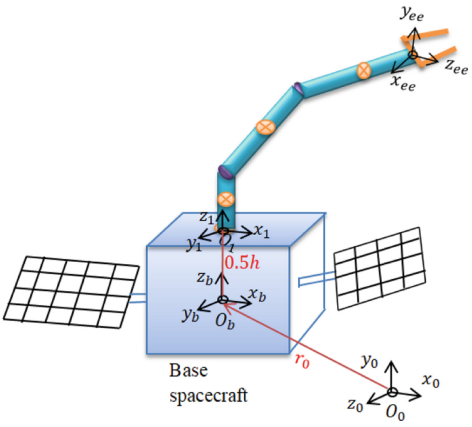

Fig. 5. Free flying space robot manipulator system

The initial configuration of space robot are given as;

$$[\phi_0, \theta_0, \psi_0]^T = [\frac{5\pi}{180}, \frac{20\pi}{180}, \frac{10\pi}{180}]^T(rad)$$

$$[x, y, z]^T = [0.11, 0.2, -0.3]^T(m)$$

$$[\theta_{10}, \theta_{20}, \theta_{30}]^T = [\frac{10\pi}{180}, \frac{10\pi}{180}, \frac{10\pi}{180}]^T(rad)$$

The final values of a FFSRMS are set to be;

$$[\phi_f, \theta_f, \psi_f] = [0, 0, 0](rad)$$

$$[x_f, y_f, z_f] = [0, 0, 0](m)$$

$$[\theta_{1f}, \theta_{2f}, \theta_{3f}] = [\frac{40\pi}{180}, \frac{60\pi}{180}, \frac{-30\pi}{180}](rad)$$

The change in mass of fuel due to thruster firing and unknown payload carried by the manipulator end-effector are considered as parametric uncertainty, as a result the mass of space robot in turn the mass and inertia parameters are also changed. For simulation the mass and inertia of link three and base spacecraft Table 2 are changed to $m_b = 90\,\mathrm{kg}, \mathrm{m}_3 = 11\,\mathrm{kg}, \mathrm{I}_0\mathrm{xx} = \mathrm{I}_0\mathrm{yy} = \mathrm{I}_0\mathrm{zz} =$

$27\,\mathrm{kgm}^2, \mathrm{I}_3\mathrm{xx} = 0.0088\,\mathrm{kgm}^2, \mathrm{I}_3\mathrm{yy} = 0.88\,\mathrm{kgm}^2, \mathrm{I}_3\mathrm{zz} = 0.88\,\mathrm{kgm}^2$. The disturbance force or torques are chosen as [30].

$$\tau_{dm} = [0.1sin(1.2t), 0.108sin(0.1t), -0.1sin(0.6t)]$$

$$\tau_{db} = [0.4sin(0.3t), 0.3cos(0.1t), 0.2sin(0.3t)]$$

$$f_b = [0.1sin(0.3t), 0.01cos(0.1t), 0.02sin(0.3t)]$$

Where, τ_{db},f_b,τ_{dm} are disturbance force & torque on the base spacecraft positions, attitudes and manipulator joints respectively. The parameter of controller are selected by trail and error method which fulfill our desired objectives. $K_p = 3I_{9,9}$,$K_i = 1.5I_{9,9}$,$K_s = 2I_{9,9}$,$G = 0.1I_{9,9}$.

Figure 6 shows the desired base spacecraft position, orientation and manipulator joint angle trajectories planned using fifth order polynomial path planning technique. The manipulator joint angles and the base spacecraft positions & orientations as well as the end effector position trajectory tracking capability with an initial errors are shown in Fig. 7. The result indicates the manipulator joint angles track their desired trajectories and the base spacecraft positions and attitudes are re-oriented at their target location (zero). Figure 7d depicts that the end effector successfully follow the prescribed path in Cartesian space. The simulation results in Fig. 7b & 7c are used to demonstrate the situation in which the base spacecraft must change its attitude or position to re-orient the earth pointing antenna so as not to loss ground communication or to keep the solar panel aligned with the sun for maximum power.

Due to an initial deviation of the system states, the manipulator joint torques as well as, the base spacecraft thrust forces & attitude torques are high initially, as shown in Fig. 8a, 8b, 8c respectively. However, the magnitude of this manipulator and base spacecraft torques and forces are bounded within $\pm 0.5\,\mathrm{Nm}$, $\pm 2\,\mathrm{Nm}$ and $\pm 1\,\mathrm{N}$ as shown in Fig. 8 respectively at steady state. Practically the base spacecraft attitudes are controlled by either reaction or moment wheel and they have limited torque up to $\pm 5\,\mathrm{Nm}$ & $\pm\,1\,\mathrm{Nm}$ respectively. Thus, the result confirms this reality.

Figure 9 shows the sliding surface are asymptotically converges to the origin and staying there over time. Therefore, all the states of the system (errors in this case) are attracted to it and stay along with the slide surface.

Figure 10 shows the trajectory tracking errors of the manipulator joint angles and the base spacecraft position & orientation angles as well as the thrust forces and torques of the system due to the addition of external disturbances.

Figure 11 shows the control torques and thrust forces of the system with FSMC & SMC. This results indicate that SMC has chattering problem. However, this problem is solved by employing a fuzzy logic controller along with SMC, as shown in Fig. 11. Table 4 shows the integral of time multiplied by absolute error (ITAE) of the system with nominal model, disturbance and parametric variation of both controller. The proposed controller has a relatively smaller ITAE than the sliding mode controller, as indicated in Table 4. Thus, the results show that FSMC has better trajectory tracking performance than SMC.

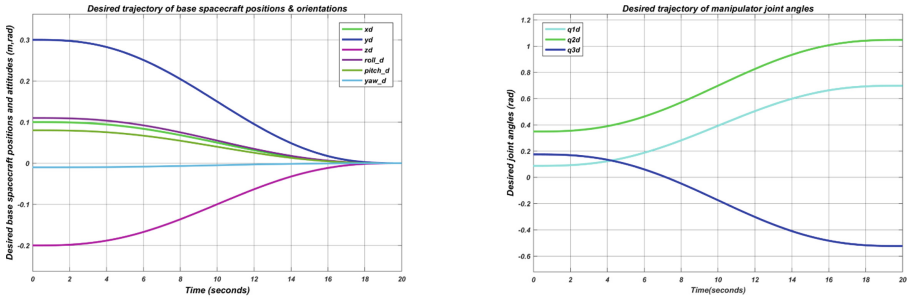

(a) (b)

Fig. 6. The desired trajectory of base position and attitude as well as the manipulator joint angle designed using fifth order polynomial path planning technique:(a) Desired trajectory of spacecraft position and attitude (b) Desired joint angle trajectory

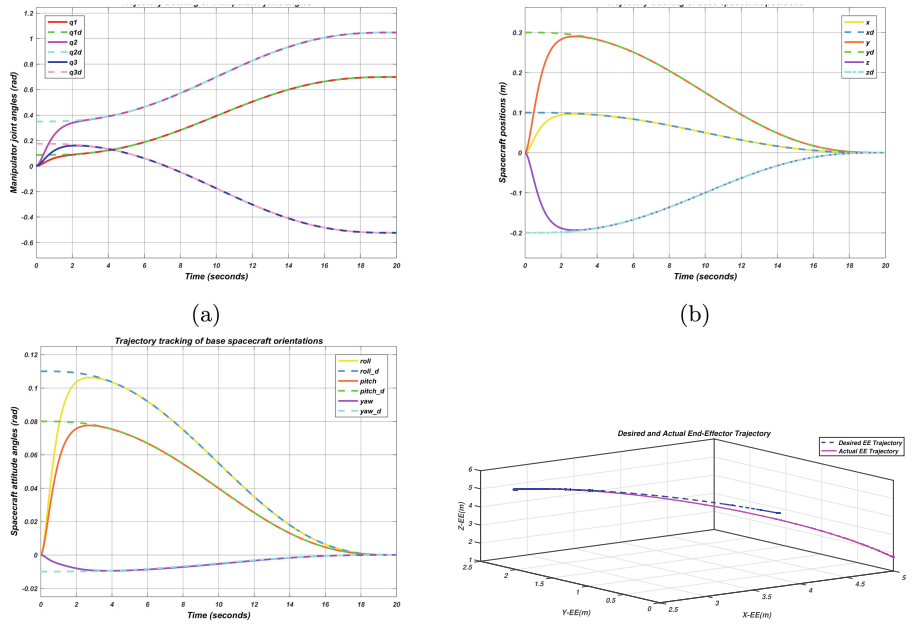

(a) (b)

(c) (d)

Fig. 7. Manipulator joint angles and Base spacecraft position & orientation and end effector trajectory tracking:(a) Manipulator joint angles trajectory tracking (b) Base spacecraft position trajectory tracking (c) Base spacecraft orientation trajectory tracking (d) end effector trajectory tracking

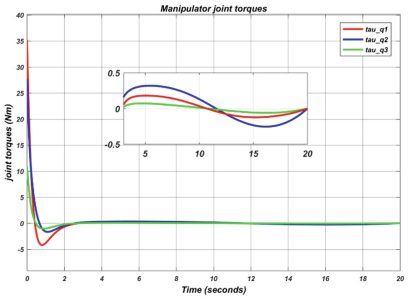

(a)

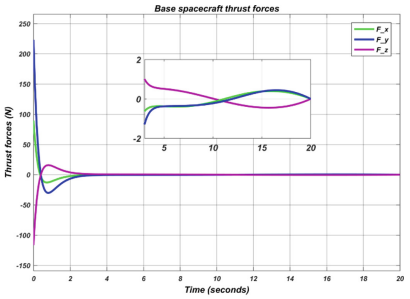

(b)

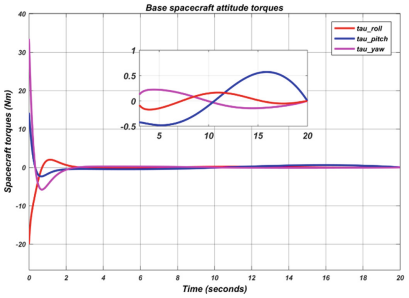

(c)

Fig. 8. Manipulator joint angle and base spacecraft torques & forces:(a) Manipulator joint angle torques (b) base spacecraft thrust forces (c) base spacecraft torques

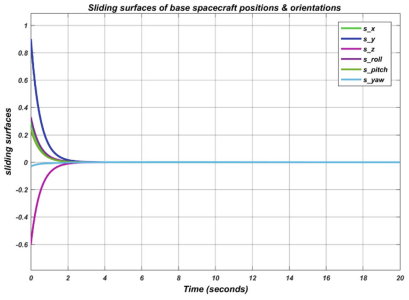

(a)

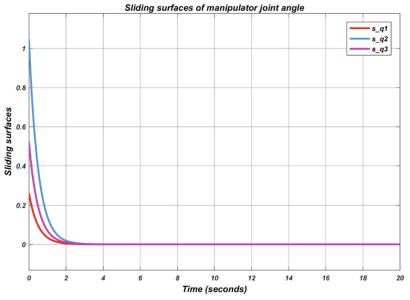

(b)

Fig. 9. Sliding surface of the base spacecraft positions and orientations and the manipulator joint angles:(a) Sliding surface of spacecraft positions and orientations (b) Sliding surface of the manipulator joint angles

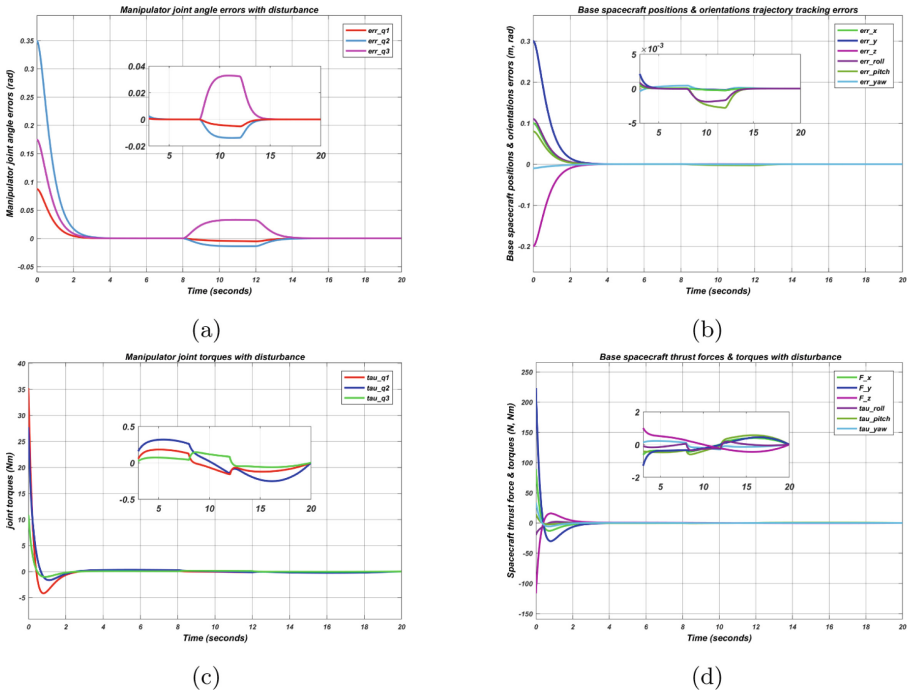

Fig. 10. Manipulator joint angle and base spacecraft position & attitude angle errors and the corresponding torques & forces with disturbance (a)Manipulator joint angle errors (b) base spacecraft position errors (c) Manipulator joint torques (d) base spacecraft forces & torques

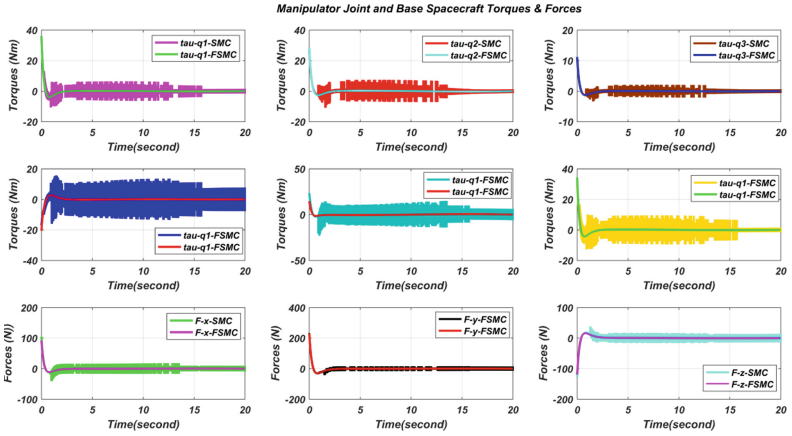

Fig. 11. Manipulator joint and base spacecraft torques & forces with FSMC & SMC

Table 4. ITAE for a FFSRMS with FSMC

	$x(m)$	$y(m)$	$z(m)$	$\phi(rad)$	$\theta(rad)$	$\psi(rad)$	$\theta_1(rad)$	$\theta_2(rad)$	$\theta_3(rad)$
FSMC-nominal	5.052×10^{-2}	1.516×10^{-1}	1.010×10^{-1}	5.752×10^{-2}	4.174×10^{-2}	2.822×10^{-2}	4.409×10^{-2}	1.763×10^{-1}	8.817×10^{-2}
SMC-nominal	6.933×10^{-2}	2.284×10^{-1}	1.482×10^{-1}	7.825×10^{-2}	5.425×10^{-2}	1.586×10^{-2}	5.951×10^{-2}	2.680×10^{-1}	1.229×10^{-1}
FSMC-disturbance	5.568×10^{-2}	1.553×10^{-1}	1.080×10^{-1}	1.005×10^{-1}	1.055×10^{-1}	2.224×10^{-2}	1.745×10^{-1}	5.247×10^{-1}	9.796×10^{-1}
SMC-disturbance	6.935×10^{-2}	2.284×10^{-1}	1.482×10^{-1}	8.314×10^{-2}	8.443×10^{-2}	1.570×10^{-2}	1.820×10^{-1}	7.333×10^{-1}	1.453×10^{0}
FSMC-parametric change	5.607×10^{-2}	1.676×10^{-1}	1.109×10^{-1}	6.019×10^{-2}	4.459×10^{-2}	2.659×10^{-2}	9.721×10^{-2}	2.232×10^{-1}	1.650×10^{-2}
SMC-parametric change	6.627×10^{-2}	2.164×10^{-1}	1.402×10^{-1}	7.520×10^{-2}	5.138×10^{-2}	1.525×10^{-2}	5.607×10^{-2}	2.464×10^{-1}	1.337×10^{-1}

6 Conclusion

In this paper a fuzzy sliding mode controller for trajectory control of a free flying space robot manipulator system was studied. The dynamics and kinematics of a the system has been formulated. A fuzzy logic controller is employed to substitutes the switching control algorithm, which causes for a chattering problem in SMC. To see the effectiveness of the proposed controller, simulation is conducted using MATLAB and it is compared with sliding mode controller. The result shows that, the proposed controller has better trajectory tracking performance and it is robust. The comparative study shows that FSMC has a reduced ITAE than SMC. Furthermore, the proposed controller(FSMC) has successfully eliminates the chattering problem. However, in this paper the coriolis /centerifugal matrix are computed following Euler-Lagrangian equation of motion which is not computational efficient. In the future, we will develop the same controller for dual arm free flying space robot system, which has a great capability to perform a complex tasks than a single arm.

References

1. Ding, X.L., Wang, Y.C., Wang, Y.B., Kun, X.: A review of structures, verification, and calibration technologies of space robotic systems for on-orbit servicing. Sci. Chin. Technol. Sci. **64**(3), 462–480 (2021)
2. Guang, Z., Heming, Z., Liang, B.: Attitude dynamics of spacecraft with time-varying inertia during on-orbit refueling. J. Guid. Control. Dyn. **41**(8), 1744–1754 (2018)
3. Li, W.J., Cheng, D.Y., Liu, X.G., et al.: On-orbit service (OOS) of spacecraft: a review of engineering developments. Prog. Aerosp. Sci. **108**, 32–120 (2019)
4. Mark, C.P., Kamath, S.: Review of active space debris removal methods. Space Policy **47**, 194–206 (2019)
5. Yoshida, K.: ETS-VII flight experiments for space robot dynamics and control. In: Rus, D., Singh, S. (eds.) Experimental Robotics VII. Lecture Notes in Control and Information Sciences, vol. 271, pp. 209–218. Springer, Berlin (2001). https://doi.org/10.1007/3-540-45118-8_22
6. https://www.nasa.gov/mission_pages/station/research/news/rrm_practice.html
7. Ogilvie, A., Allport, J., Hannah, M., Lymer, J.: Autonomous satellite servicing using the orbital express demonstration manipulator system. In: Proceedings of the 9th International Symposium on Artificial Intelligence, Robotics and Automation in Space (i-SAIRAS 2008), Los Angeles (2008)

8. Flores-Abad, A., Ma, O., Pham, K., Ulrich, S.: A review of space robotics technologies for on-orbit servicing. Prog. Aerosp. Sci. **68**, 1–26 (2014)
9. Mohamed, A., Saaj, C., Seddaoui, A., Nair, M.: Linear controllers for free-flying and controlled-floating space robots: a new perspective. Aeronaut. Aerosp. Open Access J. **4**(3), 97–114 (2020)
10. Gu, Y.-L., Yangsheng, X.: A normal form augmentation approach to adaptive control of space robot systems. Dyn. Control **5**(3), 275–294 (1995)
11. Parlaktuna, O., Ozkan, M.: Adaptive control of free-floating space robots in Cartesian coordinates. Adv. Rob. **18**(9), 943–959 (2004)
12. Xu, Y., Shum, H.-Y., Kanade, T., Lee, J.-J.: Parameterization and adaptive control of space robot systems. IEEE Transa. Aerosp. Electr. Syst. **30**(2), 435–451 (1994)
13. Abiko, S., Hirzinger, G.: Adaptive control for a torque controlled free-floating space robot with kinematic and dynamic model uncertainty. I:n 2009 IEEE/RSJ International Conference on Intelligent Robots and Systems, pp. 2359–2364. IEEE (2009)
14. Xie, L., Yu, X., Chen, L.: Robust fuzzy sliding mode control and vibration suppression of free-floating flexible-link and flexible-joints space manipulator with external interference and uncertain parameter. Robotica **40**(4), 1–23 (2021)
15. Liu, Y., Yan, W., Zhang, T., Yu, C., Tu, H.: Trajectory tracking for a dual-arm free-floating space robot with a class of general non-singular predefined-time terminal sliding mode. IEEE Trans. Syst. Man Cybern.: Syst. 52(5), 3273-3286 (2021)
16. Zhang, X., Liu, J., Gao, Q., Zhaojie, J.: Adaptive robust decoupling control of multi-arm space robots using time-delay estimation technique. Nonlinear Dyn. **100**(3), 2449–2467 (2020)
17. Jia, S., Shan, J.: Continuous integral sliding mode control for space manipulator with actuator uncertainties. Aerosp. Sci. Technol. **106**, 106192 (2020)
18. Wilde, M., Kwok Choon, S., Grompone, A., Romano, M.: Equations of motion of free-floating spacecraft-manipulator systems: an engineer's tutorial. Front. Rob. AI **5**, 41 (2018)
19. Markley, F.L., Crassidis, J.L.: Fundamentals of Spacecraft Attitude Determination and Control, vol. 1286. Springer, Cham (2014)
20. Longman, R.W., Lindberg, R.E., Zedd, M.F.: Satellite mounted robot manipulators - new kinematics and reaction moment compensation. Int. J. Rob. Res. **6**(3), 87–103 (1987)
21. Vafa, Z., Dubowsky, S.: On the dynamics of manipulators in space using the virtual manipulator approach. In: 1987 IEEE International Conference on Robotics and Automation, pp. 579–585 (1987)
22. Schaub, H., Junkins, J.L.: Analytical Mechanics of Aerospace Systems, 4th edn. AIAA Education Series, USA (2002)
23. Siciliano, B., Sciavicco, L., Villani, L., Oriolo, G.: Robotics. Springer-Verlag, London (2010)
24. Hughes, P.C.: Spacecraft Attitude Dynamics. Dover Publications, Mineola, NY (2004)
25. Spong, M.W., Hutchinson, S., Vidyasagar, M.: Robot Modeling and Control. John Wiley and Sons, New York (2006)
26. Edwards, C., Spurgeon, S.: Sliding Mode Control: Theory and Applications. CRC Press, Boca Raton (1998)
27. Holkar, K.S., Waghmare, L.M.: Sliding mode control with predictive PID sliding surface for improved performance. Int. J. Comput. Appl. **78**, 1–5 (2013)
28. Congqing, W., Pengfei, W., Xin, Z., Xiwu, P.: Composite sliding mode control for a free-floating space rigid-flexible coupling manipulator system. Int. J. Adv. Rob. Syst. **10**(2), 124 (2013)

29. Wang, X., Shi, L., Katupitiya, J.: Coordinated control of a dual-arm space robot to approach and synchronise with the motion of a spinning target in 3D space. Acta Astronaut. **176**, 99–110 (2020)
30. Zhang, Z., Li, X., Wang, X., Zhou, X., An, J., Li, Y.: TDE-based adaptive integral sliding mode control of space manipulator for space-debris active removal. Aerospace **9**(2), 125 (2022)